General Disclaimer

One or more of the Following Statements may affect this Document

- This document has been reproduced from the best copy furnished by the organizational source. It is being released in the interest of making available as much information as possible.

- This document may contain data, which exceeds the sheet parameters. It was furnished in this condition by the organizational source and is the best copy available.

- This document may contain tone-on-tone or color graphs, charts and/or pictures, which have been reproduced in black and white.

- This document is paginated as submitted by the original source.

- Portions of this document are not fully legible due to the historical nature of some of the material. However, it is the best reproduction available from the original submission.

X-611-68-443
PREPRINT

NASA TM X-63446

A GAMMA RAY TELESCOPE UTILIZING LARGE AREA WIRE SPARK CHAMBERS

R. W. ROSS
C. H. EHRMANN
C. E. FICHTEL
D. A. KNIFFEN
H. B. ÖGELMAN

NOVEMBER 1968

GSFC
GODDARD SPACE FLIGHT CENTER
GREENBELT, MARYLAND

X-611-68-4

A GAMMA RAY TELESCOPE UTILIZING LARGE AREA WIRE SPARK CHAMBERS

R. W. Ross
C. H. Ehrmann
C. E. Fichtel
D. A. Kniffen
H. B. Ogelman

November 1968

GODDARD SPACE FLIGHT CENTER
Greenbelt, Maryland

ABSTRACT

A second generation gamma-ray telescope has been developed for further experiments in balloon-borne astronomy. This instrument is composed of 32 wire-grid spark chamber modules, each $50 \times 50\ cm^2$, utilizing two-coordinate ferrite core readout. The detector is flown on a 27 million cubic foot research balloon in a search for discrete gamma-ray sources and supernovae explosions.

CONTENTS

ILLUSTRATIONS

A GAMMA RAY TELESCOPE UTILIZING LARGE AREA WIRE SPARK CHAMBERS

INTRODUCTION

Recent experiments in gamma-ray astronomy have confirmed theoretical prediction by setting upper limits on the flux of several possible discrete sources of gamma-rays of 10^{-4} to 10^{-5} /cm^2-sec. While an apparently diffuse source emitting a positive flux of this order has been reported from the region of the galactic center[1], no verified point sources have been discovered as yet. Thus, it is essential to construct an apparatus with considerably improved sensitivity. To achieve this within the duration of a single high altitude balloon flight requires a detector with greatly increased collection area. In addition, an apparatus with an area of 10^3 cm^2 or so makes possible the experimental test of a recent theoretical prediction of the emission of a rapid pulse of high energy electromagnetic radiation during the initial phase of a supernova[2]. To this end our group has developed a gamma-ray telescope utilizing a ferrite-core digitized spark chamber of 2.5×10^3 cm^2 area, an order of magnitude increase over our previously reported detector[3].

EXPERIMENT CRITERIA

The study of celestial gamma-rays remains one of the most promising areas of cosmic-ray physics and one of the more difficult. Gamma radiation from astrophysical sources would provide an excellent tool, unaltered by local or interstellar magnetic fields, for investigating many of the major energy transfer mechanisms in the universe; thereby shedding some light on the question of the origin of the charged cosmic-rays. The difficulty lies primarily in the low flux levels predicted. Experiments to date have succeeded in setting upper limits to the gamma-ray flux from most possible point sources, however no statistically significant flux of gamma radiation has been detected from a discrete stellar source.

Search for Discrete Sources of High Energy Gamma-Rays

In discussing an improved detection system, it is valuable to first look at the experiment requirements and constraints. A useful quantity for this purpose is the signal-to-noise ratio at the detector for gamma radiation from a point source[4]:

$$\frac{S}{\sqrt{N}} = \frac{I_s}{\theta} \left(\frac{\alpha A t f}{\pi I_{bg}} \right)^{1/2}$$

where I_s is the gamma-ray intensity from the source, and θ the angular resolution of the detector; α is the efficiency for detecting gamma-rays, A the sensitive area of the apparatus, t the time the source is within view, and f is the percent live time for the instrument. Also, I_{bg} is the diffuse background gamma-ray intensity, primarily from atmospheric secondaries at balloon altitude.

In the energy range of 30 - 500 MeV chosen for this experiment, the dominant conversion interaction is pair production. To obtain a high detection efficiency α it is necessary to use a large fraction of a radiation length of a high-Z material as a converter; however coulomb scattering of the electrons in a single piece converter would degrade the angular resolution θ. It is therefore desirable to distribute many thin converters through the apparatus. Doing this, one obtains the added feature of energy measurement by analysis of the multiple coulomb scattering of the pair through the thin converters.

The area-time product may be optimized by utilizing the largest practical instrument and maintaining the expected source in view for as long as possible. The percent live time factor f establishes a definite constraint on the detector size—when the event rate is such that the electronics are busy a large fraction of the time then any increase in area A brings a corresponding decrease in live time f, thus no effective gain. Other factors which may reduce live time are: an overly large acceptance solid angle, extraneous high-Z material outside the experiment aperture but within the acceptance angle, charged particle veto inefficiency, and of course long electronics cycle time.

The diffuse gamma-ray background I_{bg} may be reduced somewhat, on balloon-borne experiments, by achieving a high altitude and flying at a latitude with a high geomagnetic cutoff.

Search for Supernovae

A companion experiment to be performed by the same instrument is a test of the prediction of a very short high energy electromagnetic pulse associated with the explosive phase of a supernova[5]. The signal from such a burst of photons would be given by:

$$S = \frac{I_{sn}}{\tau_{sn}} (\alpha A \tau_a)$$

where I_{sn} is the total gamma-ray flux at the top of the atmosphere from the supernova pulse, τ_{sn} is the duration of the pulse, predicted to be on the order of tens of microseconds, τ_a is the sensitive time of the apparatus, and α and A are as previously defined. If a signal of two or more detected pairs from a

source angle $\Omega = \pi\theta^2$ and within τ_a are required for the identification of a supernova event, then the noise contribution from charged particles and diffuse background gamma-rays is negligible.

Clearly, in this detection mode the requirements for efficient conversion and large instrument area remain quite important. In addition, the detector must have a sensitive time of comparable length to the expected supernova pulse duration and a means of triggering on the occurrence of a multiple photon event must be provided.

DESCRIPTION OF THE DETECTOR

A schematic diagram of the gamma-ray telescope is shown in Figure 1. The detector consists of two separate pressure chambers. The upper pressure vessel encloses the spark chamber, high voltage circuits, some spark chamber readout electronics, and intermediate scintillators and light pipes. The lower pressure housing which maintains a laboratory environment holds the photomultipliers; high voltage power supplies; readout, coincidence and telemetry formatting electronics.

The Spark Chamber

The spark chamber is assembled from 32 independent spark modules, each constructed by stretching 0.18 mm diameter beryllium-copper wires over a frame of glass-bonded mica. The active area of this module is 50 cm by 50 cm. All modules but the bottom are wired with two orthogonal sets of 400 wires, one set on each side of the frame. The spacing between the wire grids is 4.0 mm and the distance between wires in a common plane is about 1.2 mm. The last module on the bottom of the stack contains wires arranged at 45° with respect to the wires in the remainder of the modules. This is necessary to resolve the ambiguity of properly associating two or more x readings with corresponding y readings. The occurrence of a spark causes current to flow through two or more orthogonal grid wires setting a ferrite core on the end of each grid wire, thus recording the x-y position of the spark. The cores and some of the electronic circuits needed for core interrogation are located on shelves attached to two sides of the spark module. Since a high potential difference is applied between the two grids, the core shelves are conformally coated with a silicone elastomer. A prolonged high temperature curing is utilized to minimize outgassing from this compound. A single x-y module is shown in Figure 2.

A stainless steel pair converting plate 0.56 mm (0.03 radiation lengths) thick is included between each of the top 11 spark modules. This thickness was chosen to maintain total photon conversion efficiency of about 0.2 while not introducing

significant degradation of angular resolution from coulomb scattering. The lower 19 stainless steel plates, each 0.38 mm (0.02 radiation lengths) thick, both serve for pair conversion and as scattering cells for obtaining information on the electron momentum.

The upper pressure vessel housing the spark chamber is pressurized to one atmosphere with a mixture of commercial spark chamber gas (90% Ne, 10% He) with 1% argon and about 1% ethanol. The ethanol is necessary to suppress satellite sparks produced by photo-electrons originating from the initial spark. When pulsed with a peak voltage of 1.8 kv, the spark chamber operates with an efficiency for detection of single-tracks of about 97% and an average spreading of 3 wires per spark. The double track efficiency, which is also nearly 97%, has been enhanced by including a 22 ohm resistor in series with each high voltage grid wire. This resistance tends to decouple the wire touched by the initial spark from the rest of the grid. A thorough treatment of spark module characteristics may be found in reference 3.

The sensitive time of the spark chamber is a parameter of particular importance to the supernova experiment. Tests were performed with a spark chamber using a gas fill as previously described and no clearing field to determine the efficiency for detecting single particles vs delay of the high voltage pulse. It was found that for delays up to five microseconds the efficiency fell no lower than 20%. A sensitive time of five microseconds should be adequate for the supernova requirement, while not so large as to allow sparking on old charged particle tracks which occur at an average interval of about 100 microseconds at balloom altitudes.

The Coincidence-Anticoincidence System

The coincidence-anticoincidence system consists of three components—the B scintillator array, the Cerenkov counter, C, and the A scintillator dome. The function of these components in each of the two experiment modes will be discussed in the electronics section.

The B array is composed of nine elements, each a 0.48 cm by 16.5 cm square piece of Pilot M scintillator solvent bonded to an adiabatic plexiglas light pipe. These solvent bonds represent considerable structural improvement over the epoxy bonds used in the past with no sacrifice in optical quality. Measurements on test bonds of Pilot M to plexiglas have shown tensile strengths of about 1200 psi. While scintillator to PVT (scintillator base plastic) bonds appear to be somewhat stronger, plexiglas was chosen for the light pipes because of its lower light attenuation characteristics. These light pipes direct the scintillator output through a window sealed in the pressure bulkhead to a phototube in the lower chamber.

The nine Cerenkov counters are 5 cm by 16.5 cm square blocks of UVT Plexiglas optically bonded to the face of either a 12.7 cm diameter or 19 cm diameter photomultiplier tube, depending on the location. These counters are made unidirectional by painting the top surface black to discriminate against the upward moving cosmic-ray albedo.

The anticoincidence counter is a highly polished single-piece casting of Nuclear Enterprises 110 scintillator, measuring 1.2 m inside diameter at the bottom, 0.81 m high and averages 2 cm thickness. Aluminum foil and blackened epoxy are used as an outer covering. The scintillator is viewed by 18 phototubes spaced evenly around the lower lip. This geometry and material were chosen to optimize light collection; hence efficiency for vetoing charged cosmic-rays.

Detector Electronics

The organization of the detector electronics is shown schematically in Figure 3. The major constituents of the system are the coincidence electronics, the supernova multiscalers, and the spark chamber readout electronics.

The coincidence system itself may be broken down into two modes of operation; the telescope mode in which single photon events, as may be associated with point source astronomy, are detected, and the hodescope mode which is utilized for the supernova experiment. As may be seen in Figure 4, these experiment modes may be operated simultaneously or individually.

The overall coincidence telescope is made up of nine individual telescopes, each composed of an intermediate scintillator tile B_i and the Cerenkov counter C_i directly beneath. In addition to the obvious advantage of redundancy, this arrangement restricts the acceptance solid angle more than would a single scintillator and single Cerenkov counter telescope. Since to be acceptable a photon must pass through the topmost spark chamber module active area, any increase in solid angle causes a reduction of live time with no significant increase in detection efficiency. The $\Sigma B_i C_i$ signal may be vetoed by the anticoincidence, thus indicating the accuating particle was not neutral, but charged; or by a readout busy signal, which prevents the spark chamber being fired again before readout is complete.

For the supernova detection experiment, a slightly different triggering logic is necessary. The A counter cannot be used since in an intense gamma-ray pulse, some of the photons will convert in the residual atmosphere above the detector or in the counter itself, thereby rejecting the event. The function of the guard scintillator, rejecting the charged particle background, is accomplished by requiring that several particles are detected by the B and C counters within a short period. In particular, the requirement is that any three C tiles and any

two B tiles register charged particle passage within a period of 5 μsec. This interval, τ_s , was chosen from considerations previously discussed. Since the arrangement gives a change triggering rate of only 0.1 cpm or so, thus no significant loss of live time, both experiment modes are operative at one time.

To gain information regarding the time profile of the supernova pulse, two sets of multiscalers are incorporated into the experiment electronics. The counting rates from the central B scintillator tile (B_5) and the Cerenkov counter (C_5) are monitored during four time increments (0-20 μs, 20-80 μs, 80-320 μs, 320-1280 μs). The multiscalers are started whenever the scintillator-Cerenkov hodescope detects a supernova-type event.

The electronics for scanning the 25, 200 core spark chamber memory consists of 10 reset current sources operating in conjunction with 320 grounding circuits and 32 sense amplifiers. For each core shelf a current source provides a reset pulse through one of 5 groups of 16 cores selected by one of 5 grounding circuits on the shelf. A set core in that group is then detected by one of the 16 sense amplifiers serving each half of the chamber. The outputs from all the sense amplifiers are transferred to a 32 bit shift register. The configuration of the current source-grounding circuit select matrix in conjunction with the bit position in the shift register uniquely specifies one coordinate of the spark. The entire spark chamber is scanned in less than one second and the spark data long with various telescope rates and housekeeping parameters are telemetered to the ground.

The assembled instrument without the anticoincidence scintillator is shown in Figure 5.

CONCLUSION

The approach adopted for this instrument was not only to design a detector with greatly improved sensitivity for balloon-borne astronomy, but also to utilize, as much as possible, the opportunity for testing concepts which might be applied to a satellite instrument. This valuable study has encouraged us to begin design of a spark chamber gamma-ray telescope solely for space flight.

REFERENCES

1. Clark, G. W. G. P. Garmire, W. L. Kraushaar, Ap. J., 153, L203, (1968).

2. Colgate, S. A., Can. J. Phys., 46, S476, (1968).

3. Ehrmann, C. H., C. E. Fichtel, D. A. Kniffen, and R. W. Ross, Nuc. Inst. & Meth., 56, 109, (1967).

4. Greisen, K., Perspectives in Modern Physics, New York, 355, (1966).

5. Fichtel, C. E., H. B. Ogelman, NASA TN D-4732, (1968).

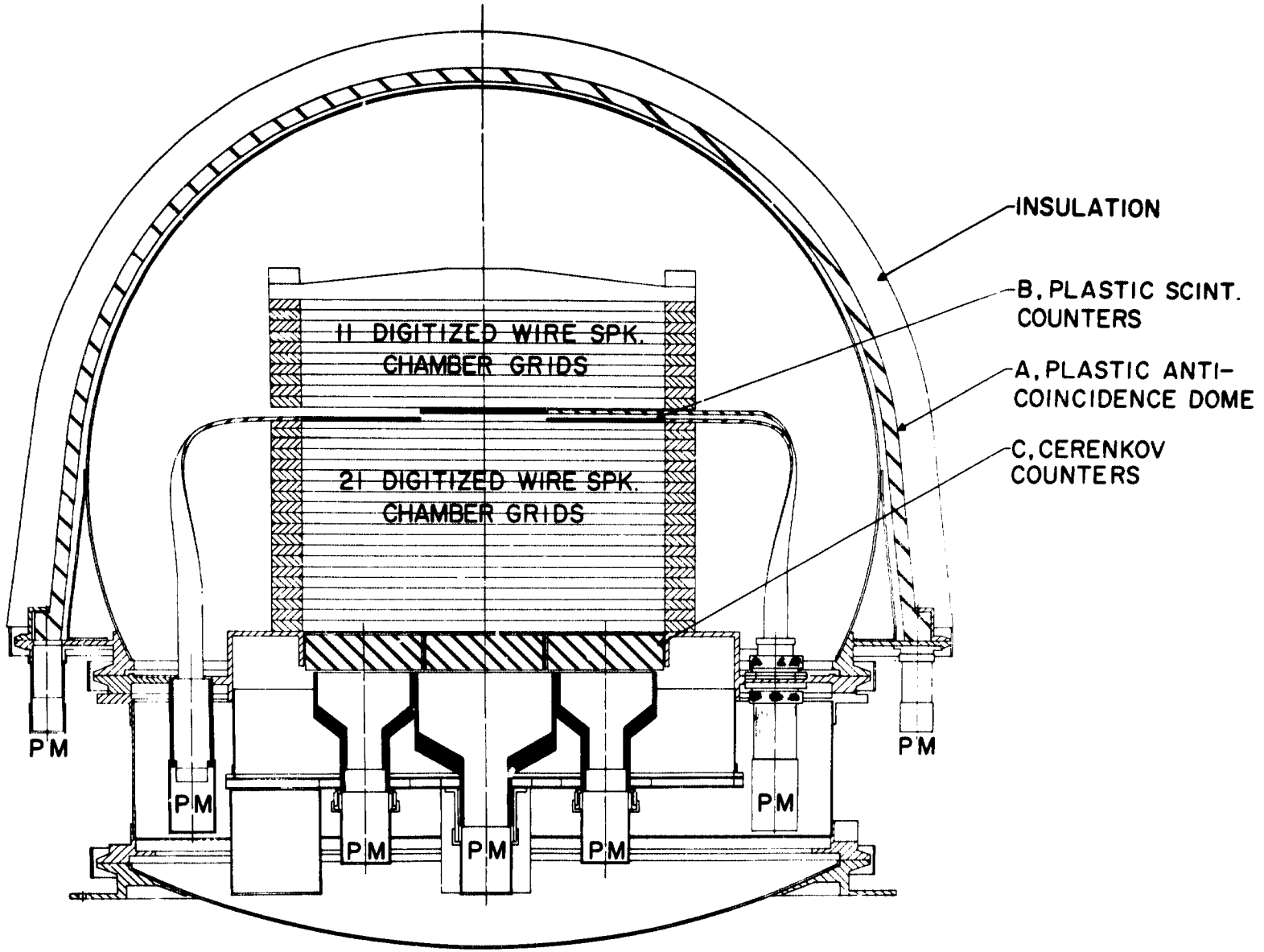

SCHEMATIC OF 1/2 x 1/2 M. DIGITIZED SPARK CHAMBER GAMMA RAY TELESCOPE

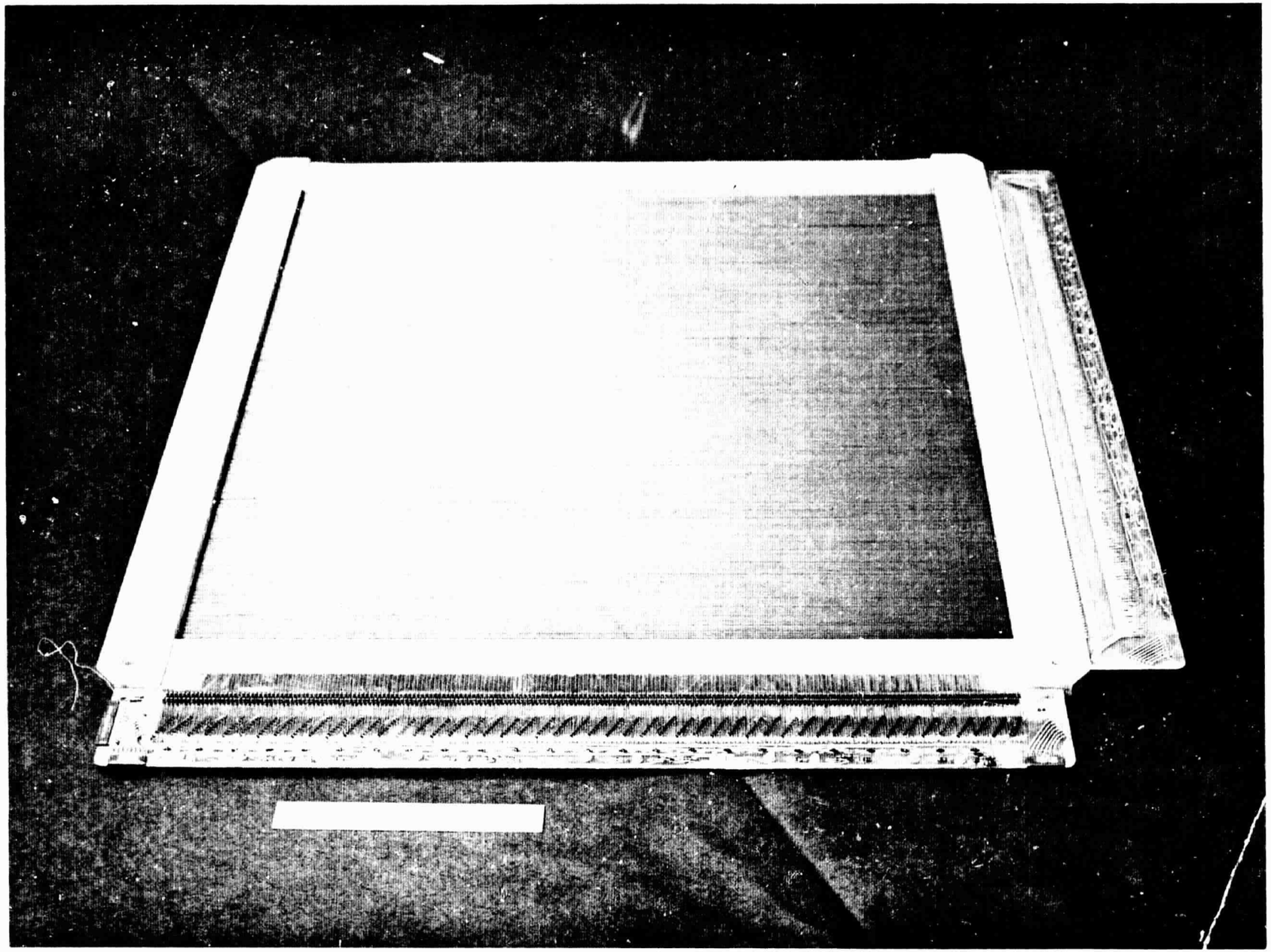

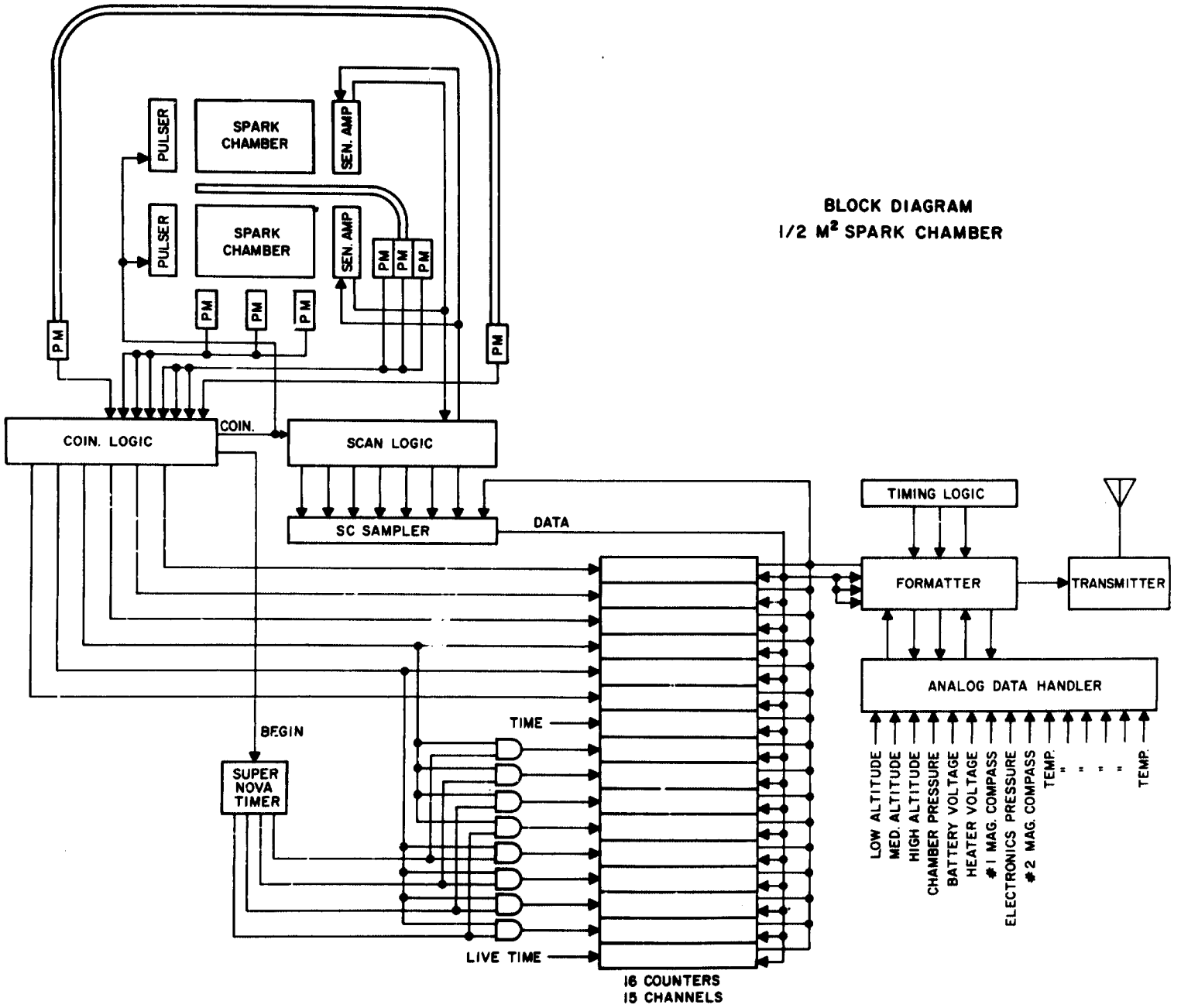
BLOCK DIAGRAM
1/2 M² SPARK CHAMBER
PULSER
SPARK CHAMBER
SEN. AMP
PULSER
SPARK CHAMBER
SEN. AMP
PM
PM
PM
PM
PM
PM
PM
PM
PM
COIN. LOGIC
COIN.
SCAN LOGIC
SC SAMPLER
DATA
TIMING LOGIC
FORMATTER
TRANSMITTER
ANALOG DATA HANDLER
BEGIN
SUPER NOVA TIMER
TIME
LIVE TIME
16 COUNTERS
15 CHANNELS
LOW ALTITUDE
MED. ALTITUDE
HIGH ALTITUDE
CHAMBER PRESSURE
BATTERY VOLTAGE
HEATER VOLTAGE
#1 MAG. COMPASS
ELECTRONICS PRESSURE
#2 MAG. COMPASS
TEMP.
"
"
"
TEMP.

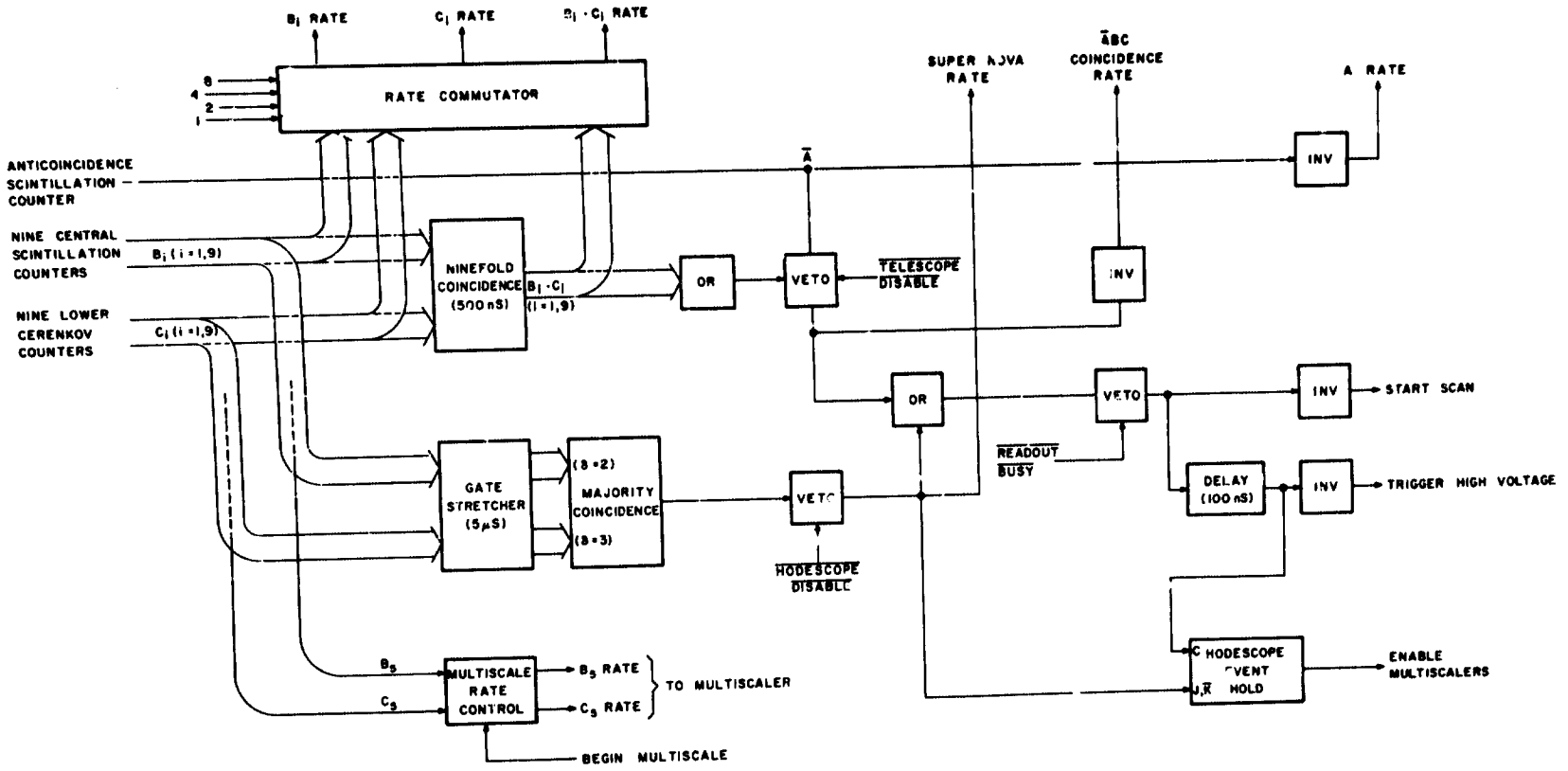

COINCIDENCE LOGIC, HALF METER GAMMA RAY EXPERIMENT